SIMULATION OF SEMICONDUCTOR DEVICES AND PROCESSES Vol. 5
Edited by S. Selberherr, H. Stippel, E. Strasser - September 1993

Simulation in High Efficiency Solar Cell Research

S. Sterk and S. W. Glunz

Fraunhofer-Institut für Solare Energiesysteme
Oltmannstr. 22, D-79100 Freiburg, GERMANY

Abstract

The practical application of numerical device simulation in high efficiency silicon solar cell research is presented. Aspects of the design development and the characterization are discussed.

1. Introduction

Two main features of high efficiency silicon solar cells [1], see Fig. 1, are high minority carrier lifetime τ_B in the bulk and low recombination velocities S_{ox} of the minority carriers at the oxidized surfaces, especially at the rear side. Since the recombination velocity S_m at the metallized surface regions is much higher, the rear side is only locally contacted.
We present an optimization study for the design of the rear point contact pattern, and advanced characterization techniques for the starting material, the interfaces and the diffused regions.

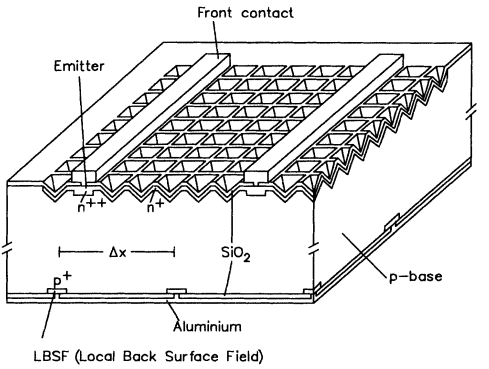

Figure 1: LBSF Solar Cell.

2. Optimization of the Rear Contact Design

Because the diffusion length L of the carriers is several times the base thickness, the total carrier loss depends strongly on the recombination at the rear surface, mainly occurring at the silicon-metal interface of the local rear contacts. In this paper we present an experimental and theoretical optimization study for the rear side point contact design (point spacing and size). The results are presented in Fig. 2.

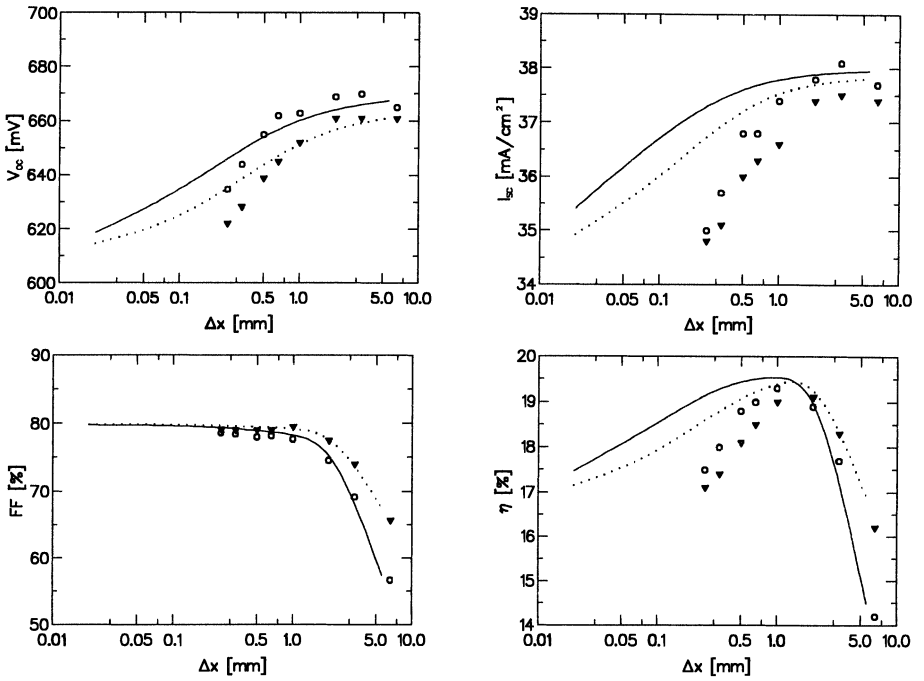

Figure 2: Simulated (lines) and measured (dots) solar cell parameters V_{oc}, I_{sc}, FF and η for two metallization fractions 4% (▾, ·····) and 0.5% (○, —) versus the contact point spacing.

Assuming low injection conditions and an ideal emitter, we solve the 3D diffusion equation for the minority carrier density [2] and the 3D Poisson equation for the electrostatic potential and the majority carrier flux [3] in the base separately. We use the Finite Differences method with a simple tensor product grid. The simulation of the minority carrier density includes photoinduced carrier generation (solar spectrum AM1.5), realistic bulk lifetimes, surface recombination velocities at the oxidized and metallized surfaces and base resistivities for commonly used solar cell materials, resulting in values for the open circuit voltage V_{oc} and the short circuit current I_{sc}. The model for the majority carrier flux includes the specific contact resistivity ρ_c and the bulk resistivity ρ_b. It computes the resistance of the base of the solar cell, mainly due to the current crowding around the point contacts, which decreases the fill factor FF of the I-V-curve of the solar cell under illumination. The efficiency η of the solar cell is given by the product of V_{oc}, I_{sc} and FF, devided by the power of the incident sun light.

We have simulated and processed solar cells with different rear contact design. The spacing Δx of the quadratic contact point pattern varies from 0.25 mm up to 6.6 mm, the metallization fraction f_m of the rear side was 4% (triangles, dotted lines) and 0.5% (circles, solid lines). The cells have been processed identically on 1.0 Ωcm p-type material, the rear contact was formed by aluminum alloying. The simulation parameters were L = 650 μm, S_{ox} = 10 cm/s, S_m= ∞, ρ_b = 1.0 Ωcm, ρ_c = $3x10^{-4}$ Ωcm^2.

Fig. 2 shows the increase of V_{oc} and I_{sc} with increasing point spacing, due to the decreasing influence of the recombination at the contacts. For $\Delta x \rightarrow 0$, the simulated V_{oc} and I_{sc} values adopt the 1D calculated limit for $S_{eff} = (1-f_m)S_{ox} + f_m S_m$ at the rear side. Because the injection level at the rear side decreases for smaller point spacing, the surface recombination velocity at the oxide increases [4]. This effect is not incorporated in the present simulation model, thus the measured I_{sc} values for the small point spacing are lower than the calculated ones.
The decrease of the fill factor with larger point spacing and smaller point size is due to the increasing series resistance. The contrary behavior of V_{oc}, I_{sc} and FF results in an maximum for η. The width, the position Δx and the height of this maximum depend strongly on the material parameters and the metallization fraction.

3. Characterization

Recombination parameters at different steps of solar cell processing are conveniently determined by contactless nondestructive measurements (e.g. IR-absorption [5], microwave reflection, photoconductivity decay). Up to now simplifying analytical models have been used for extracting parameters, but numerical models (Finite Differences method) are becoming more and more important. This is due to their flexibility in handling more complex structures (doping profiles, inhomogeneities).
We concentrate on lifetime experiments using sine amplitude modulated light (in contrast to light pulses) to generate carriers. For a simple model with a homogeneous bulk lifetime τ_b and two surface recombination velocities S_{front} and S_{back} it is easy to extract analytically the recombination parameters from the phase shift and the frequency dependent amplitude of the integrated carrier density, measured by a transmitted IR-beam or MW-reflection.
In Fig. 3 the electron density in a 200 µm thick, uniformly doped p-type wafer, calculated by a time resolved numerical method, for three modulation periods of two different frequencies is shown. Obviously for the higher frequency (100 kHz) the phase shift is higher and the amplitude of the electron density is smaller. Using light of short penetration

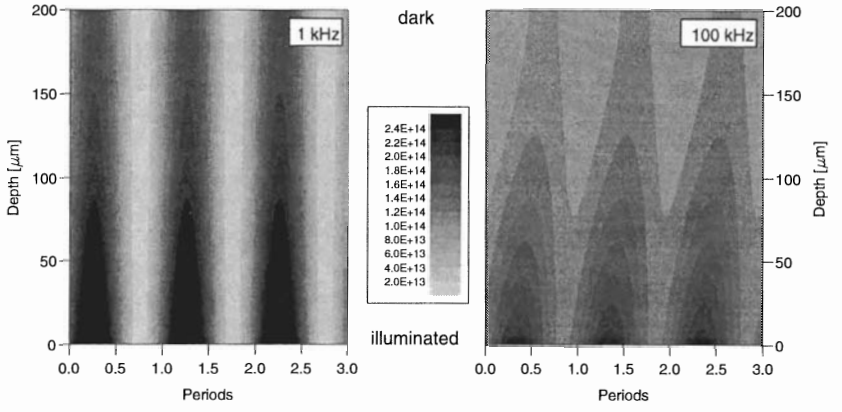

Figure 3: Density of electrons in a uniformly doped p-type wafer (200µm) illuminated with modulated light of short penetration depth (α^{-1}=1µm)

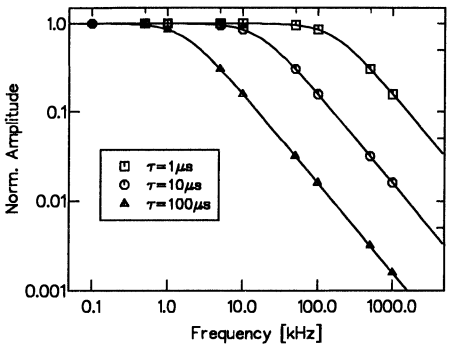

Figure 4: Comparision of analytical (solid lines) and numerical calculation.

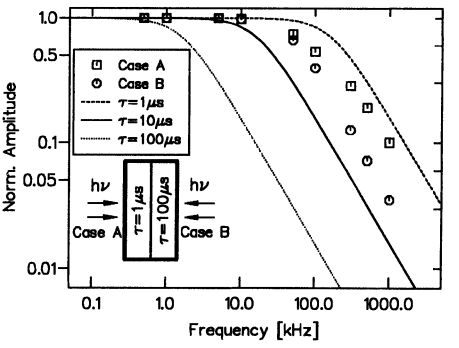

Figure 5: Two layer structure with different lifetimes.

depth (α^{-1}=1μm), the carrier modulation for the high frequency takes place mainly under the illuminated surface, due to the fact that the modulation is faster than the carrier transfer by diffusion. Thus, the surface and bulk recombination can be separated.
The calculated numerical values for this simple structure are in perfect agreement with the analytical curves, which is demonstrated in Fig. 4 for three different τ_b values.
However more complex structures such as a two-layer system with two different τ_b values (e.g., thin film solar cells, where an epitaxial layer with a high lifetime is grown on a low quality substrate) cannot be described easily by an analytical model. The numerical calculation of this structure for both illumination directions in Fig. 5 shows that no simple model for an average τ_b can be used. For both cases the shape of the amplitude follows neither the behaviour of the geometrical average τ = 10μs nor of the arithmetical average τ = 55μs. Thus, for this structure only the numerical calculation is useful to extract the recombination parameters from the experimental values.

4. Conclusion

3D device simulation with a simple model provides good qualitative understanding of the dependence of the solar cell efficiency on the contact design. The advantage of numerical evaluation in characterization of complex structures has also been outlined.

[1] J. Knobloch, A. Aberle, B. Voss, *Cost Effective Processes for Silicon Solar Cells with High Performance*, Proc. 9th E.C. PVSEC, Sept. 1989, p.777
[2] S. Sterk, *Optimization of the rear contact design of high efficiency solar cells*, to be published
[3] S. Sterk, S. Glunz, W. Warta, *Ohmic Losses in the Base of Solar Cells with Local Rear Contacts*, submitted to IEEE Trans. Electron Devices
[4] A. Aberle, S. Glunz, W. Warta, *Impact of Illumination Level and Oxide Parameters on SRH Recombination at the Si-SiO_2 Interface*, J. Appl. Phys. 71(9), 1992, p. 4422
[5] F. Sanii, R. J. Schwartz, *The Measurement of Bulk and Surface Recombination by Means of Modulated Free Carrier Absorption*, Proc. 20th IEEE PVSC, 1988, p. 575